

**Figure 4** *H*-plane radiation contour and patterns from 55 to 65 GHz

return loss and array gain. Figure 3 shows *E*-plane radiation patterns and contour plot from 55 to 65 GHz. Similarly, Figure 4 shows radiation patterns and contour for the *H* plane. Figure 5 shows the boresight gain versus frequency for the 64-element array.

Three such arrays were built, the best results are shown in the figures. The distribution was designed to feed an equal amplitude antenna array. Near side lobes varied a couple of decibels around  $-13$  dB throughout the 55–65-GHz bandwidth. Boresight half-power beam width remains nearly constant throughout the measured bandwidth. Increase in side-lobe level occurs at a couple of frequency points, which may be due to a variety of reasons, including mismatch interactions, coupling within distribution networks, and/or measurement setup. The boresight gain variation is within a couple of decibels throughout most of the bandwidth. The overall efficiency of the antenna array varies between 30 and 40%. Current research efforts are trying to assess how the losses are distributed throughout the array. The loss mechanisms include the radiator, circular waveguide–strip-line transition, distribution split-

ters, and line losses, strip-line–rectangular waveguide transition, and a WR-15 *E*-plane  $90^\circ$  bend.

#### 4. CONCLUSION

A low-profile, wide-band antenna array concept has been designed, built, and tested. The 64-element array uses rectangular waveguide, coax, strip line and circular waveguide. The radiation patterns remain fairly consistent throughout the measured bandwidth, and overall efficiency is reasonable at around 35%. The boresight gain variation is better than expected and efforts to reproduce and improve these results with the other two units are under way.

© 2002 Wiley Periodicals, Inc.

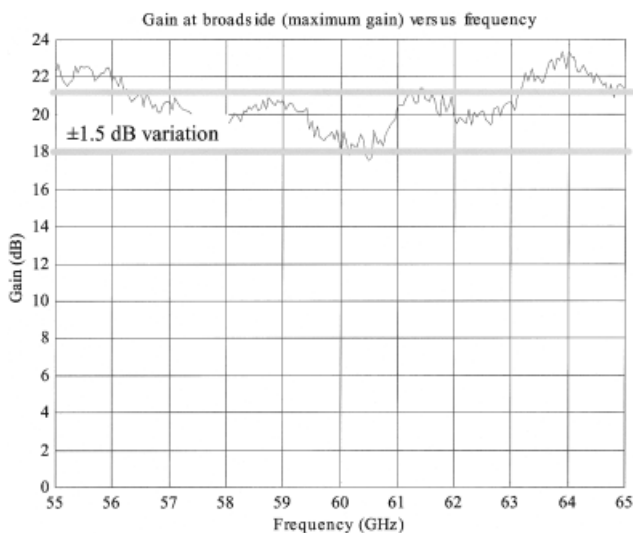


**Figure 5** Boresight gain variations from 55 to 65 GHz

## A NOVEL SUPERCONDUCTING CPW SLOW-WAVE BANDPASS FILTER

Jiafeng Zhou, Dungshing Hung, Michael J. Lancaster, Hieng Tiong Su, and Xuming Xiong

School of Electronic, Electrical and Computer Engineering  
The University of Birmingham  
Edgbaston, Birmingham B15 2TT, UK

Received 7 February 2001

**ABSTRACT:** A novel slow-wave half-wavelength coplanar waveguide (CPW) resonator using high- $T_c$  superconducting (HTS) films has been studied and used in a new filter topology. The slow-wave effect is achieved by the capacitively loaded structure with a symmetrical interdigital line loaded on both sides of the central line. The velocity reduction ( $V_p/c_0$ ) of the resonator is about 0.050. A three-pole Butterworth bandpass filter has been designed and fabricated with the use of the resonator. © 2002 Wiley Periodicals, Inc. *Microwave Opt Technol Lett* 34: 255–259, 2002; Published online in Wiley InterScience (www.interscience.wiley.com). DOI 10.1002/mop.10431

**Key words:** bandpass filter; slow wave; interdigital gap; HTS; CPW

## 1. INTRODUCTION

Because of the extremely low loss at microwave frequencies, many microwave applications of high-temperature superconductors (HTS), such as mobile and satellite telecommunications, are promising [1]. Recent developments in HTS circuits and microwave monolithic integrated circuits (MMIC) have stimulated the investigation of new planar filters. Coplanar waveguides (CPW) have been suggested as alternatives to microstrips on MMICs [2–5]. The predominant advantages of coplanar structures are that they simplify the fabrication process by using single-side deposited film and eliminating via holes in the substrate. Compared to microstrip, it is easier to insert both series and parallel components with high circuit density.

A number of CPW resonators have been studied to reduce the size and weight of the microwave structures [6–8]. Only a few superconducting slow-wave CPW filters have been reported [9, 10] to date. In this Letter the method of increasing the capacitance by using interdigital lines is used to make a novel miniature CPW resonator. It is shown that the structure enables strong coupling and enhances the loaded capacitance. The size of filters based on the resonator can be greatly reduced by using such coplanar slow-wave resonators. The unloaded Q measured at 26 K of a 1.76-GHz resonator is up to 3000. Although this is lower than some other HTS resonators, it should be noted that the resonator is extremely small. The behavior of the resonator is examined by the design and production of a third-order 8-GHz central frequency end-coupled Butterworth bandpass filter with a 2% bandwidth. The design procedure and measured performance of the filter are also described.

## 2. RESONATOR

### A. Theory

The phase velocity of slow-wave modes propagating along a transmission line is determined by the energy stored in sections of the circuit. Lumped-element circuit theory says that the phase velocity ( $V_p$ ) is dependent on both inductance per unit length ( $L$ ) and capacitance per unit length ( $C$ ) when the wave propagates along the low-loss conducting transmission line. The relationship can be expressed by

$$V_p = 1/\sqrt{LC} \quad (1)$$

As indicated in (1), changing both  $L$  and  $C$  can change the phase velocity. However, in a conventional distributed TEM transmission line,  $L$  and  $C$  are also related to each other. This would make it impossible to modify the phase velocity by changing either  $L$  or  $C$  without affecting the other. This dilemma can be overcome by replacing physically uniform lines with periodically loaded lines.

A simple way to make a slow-wave structure is to place a series of coplanar lines on the sides of a conventional half-wavelength resonator, as shown in Figure 1(a). The slow-wave resonator is composed of symmetrical coplanar interdigital structures located on both sides of the central line. The whole circuit can be regarded as a capacitively loaded slow-wave structure shown in Figure 1(b).

In the equivalent circuit, because the loaded coplanar line is capacitive, it has a characteristic impedance  $Z_1$  and capacitance  $C_1$ , and the central lines have a characteristic impedance  $Z_0$  and a propagation constant  $\gamma$ . The phase velocity of the slow-wave line can be expressed as [11]

$$V_p = 1/\sqrt{L\left(C + \frac{C_1}{d}\right)} \quad (2)$$

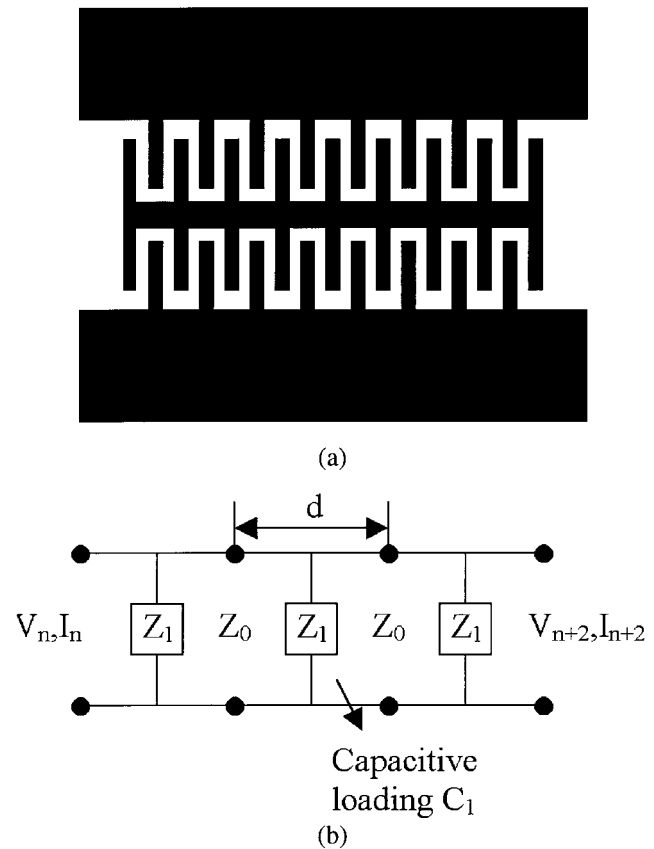


**Figure 1** (a) Coplanar slow-wave resonator, (b) the equivalent circuit of the resonator

where  $d$  is the length of each unit cell. This form implies that the capacitively loaded parallel line at low frequency (the length is much less than wavelength) behaves as an electrically smooth line with a series inductance  $L$  and a shunt capacitance  $C' = C + C_1/d$ . The decrease of the phase velocity  $V_p$  resulting from the extra capacitances  $C_1$  is caused by the capacitive loading. An expression to calculate the capacitance  $C_1$  can be found in Reference [12].

### B. Experimental Result

To measure the unloaded Q value of this kind of resonator, a superconducting coplanar resonator is designed in a  $7.96 \times 1.08$ -mm area with wide ground planes on both sides. The interdigital lines loading the central line are 0.50 mm in length and 20  $\mu\text{m}$  in width surrounding a 20- $\mu\text{m}$  gap. The circuit is made of 350-nm-thick  $\text{YBa}_2\text{Cu}_3\text{O}_7$  superconducting thin film and printed on a  $10 \times 10 \times 0.5$ -mm MgO substrate. The fundamental mode of the resonance is 1.76 GHz at 26 K. The measured response of the CPW resonator with  $-10$ -dBm input power is shown in Figure 2. The unloaded Q of the fundamental mode at different temperature and input power are illustrated in Figure 3. The measured response indicates a 0.096 velocity reduction ( $V_p/c_0$ ), where  $c_0$  is the light speed in vacuum, which leads to 90% reduction of physical length by the capacitively loaded structure, with an about 2000–3000 unloaded Q-value. Figure 3 shows the effect of increasing the microwave power to the resonator, indicating that such a resonator is mainly useful for low-power microwave applications.

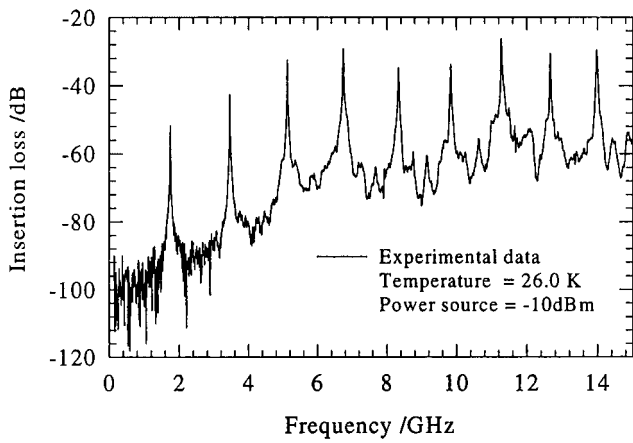


Figure 2 The measured responses of the CPW resonator

### 3. FILTER

#### A. Theory

The lump-element low-pass filter prototype is used to design the bandpass filter. The elements for Butterworth low-pass filters, and the transformation of low-pass to band-pass filters, are given in Reference [13]. The converted band-pass circuit using only shunt resonators and admittance inverters is illustrated in Figure 4.

In the practical filter the substrate is MgO with a thickness of 0.5 mm and relative dielectric constant 9.8. The impedance for the input and output ports for the circuits is designed to be  $50 \Omega$ . The loaded interdigital line width and gap are  $20 \mu\text{m}$  (central line  $40 \mu\text{m}$ ). For an 8-GHz center frequency the required lengths of resonator section with different interdigital line length are plotted in Figure 5. This is obtained by using Sonnet EM simulation software [14], which gives a velocity reduction ( $V_p/c_0$ ) up to 0.025. The length 0.48 mm is chosen in this design for the interdigital lines with a velocity reduction about 0.050.

The method to calculate the capacitance of individual resonator can be obtained in reference [12]. The procedure to extract  $J$  inverters can be found in [15]. In this design, to make the third order, 2% bandwidth end-coupled Butterworth bandpass, the required values are

$$J_0 = 4.0 \times 10^{-3}/\Omega$$

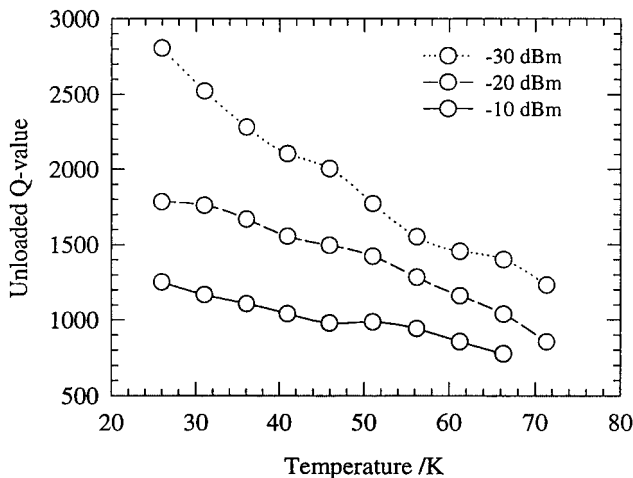


Figure 3 Unloaded Q at different temperature and input power

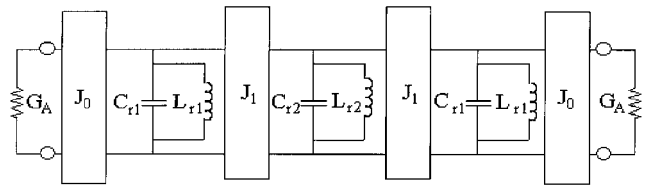


Figure 4 Equivalent circuit for the third-order lumped-element bandpass filter

$$J_1 = 5.6 \times 10^{-4}/\Omega$$

The single resonator with identical gaps on both ends of the line is used to determine the gap sizes for the required inverters. The  $J$  values are obtained by [13]

$$J = Y_c \cdot \sqrt{\frac{\pi}{2Q_c}}, \quad (3)$$

where  $Q_c$  is the external quality factor of the resonator, which may be characterized by

$$Q_c = \frac{f_0}{\Delta f_{3\text{dB}}}, \quad (4)$$

where  $f_0$  and  $\Delta f_{3\text{dB}}$  are the resonant frequency and the 3-dB bandwidth of the resonator when it is externally excited. Determination of the  $Q$  values is carried out by using Sonnet EM simulation software [14];  $Y_c$  is the admittance of the resonator, which is characterized by the calculated capacitance above as

$$Y_c = \sqrt{\frac{C + C_1/d}{L}}. \quad (5)$$

As shown by the dotted line in Figure 6, the admittance  $J$  values are given from  $5.6 \times 10^{-4}$  to  $1.9 \times 10^{-3}$  by adjusting the gap from 100 to  $20 \mu\text{m}$ . This gives the required admittance  $J_1$  ( $5.6 \times 10^{-4}$ ). However, as indicated in Figure 6, the value of  $J_0$  requires a coupled gap width much smaller than  $20 \mu\text{m}$ . It is very difficult to fabricate such circuit. As illustrated in Figure 7, the interdigital coupling structure, line width and gaps, of which are all  $20 \mu\text{m}$ , is employed at the end of the terminal resonator to implement  $J_0$ . The interdigital lines are more effective in coupling than the simple gap. As shown by dashed line in Figure 6, the

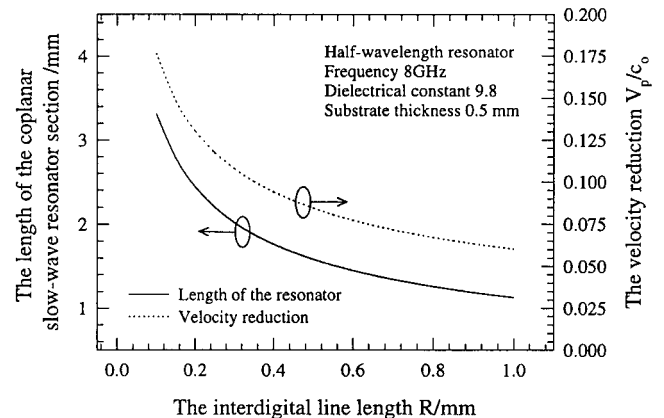
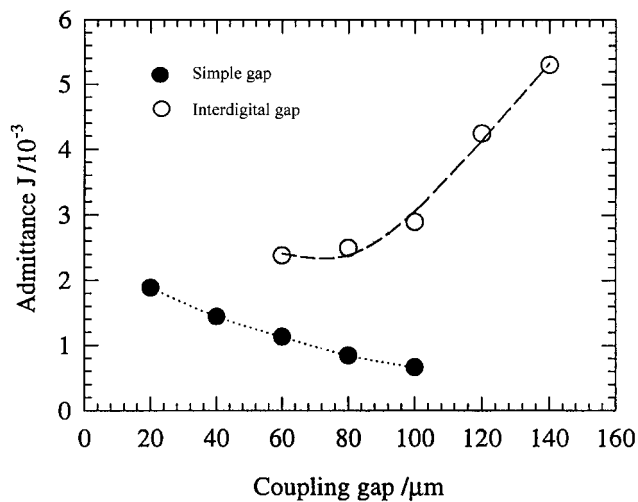


Figure 5 The resonant frequency versus the length of the CPW resonator



**Figure 6** Simulated admittance  $J$  using simple gap and interdigital gap coupling

admittance values  $J$  are obtained from  $2.4 \times 10^{-3}$  to  $5.4 \times 10^{-3}$  by changing the length of the interdigital coupling lines from 60  $\mu\text{m}$  to 140  $\mu\text{m}$ .  $J_0$  and  $J_1$  are realized by simple gap and interdigital gap with proper lengths, respectively.

The three-pole filter is finally designed in a  $5.42 \times 1.04$ -mm area, which is below  $0.39\lambda_{\text{go}}$  by  $0.07\lambda_{\text{go}}$ , where  $\lambda_{\text{go}}$  is the guided wavelength of a 50- $\Omega$  line on the substrate at the midband frequency. The layout of the circuit is shown in Figure 7. The circuit is fabricated with the use of a  $\text{YBa}_2\text{Cu}_3\text{O}_7$  thin film deposited by laser ablation on a  $10 \times 10 \times 0.5$ -mm MgO substrate. The simulated response, assuming a perfect, zero-thickness conductor and lossless substrate, is shown in Figure 8(a). As is shown, the simulated central frequency is a bit higher in frequency than the designed one of the lumped-element circuit. A similar phenomenon was also found in Reference [16]. A transmission zero is found at 7.89 GHz. This is because the dimension of the circuit is very small, and coupling exists between the first and third resonators. The relationship of the transmission zero and the coupling is described in Reference [17].

### B. Experimental Result

The circuit is measured in a brass box with K connectors, with the use of an HP 8720A network analyzer. A closed-cycle cooling system is used to cool down the whole circuit. The experimental results are shown in Figure 8. Figure 8(a) represents the pass-band details measured at temperature 30 K with  $-30$ -dBm input power. The measured central frequency is 8.09 GHz, which is 90 MHz

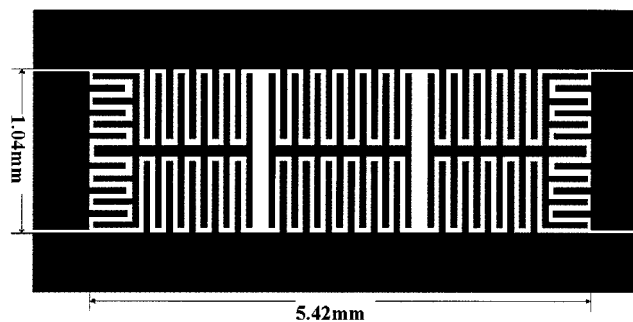


**Figure 7** Layout (not to scale) of the third-order Butterworth bandpass filter

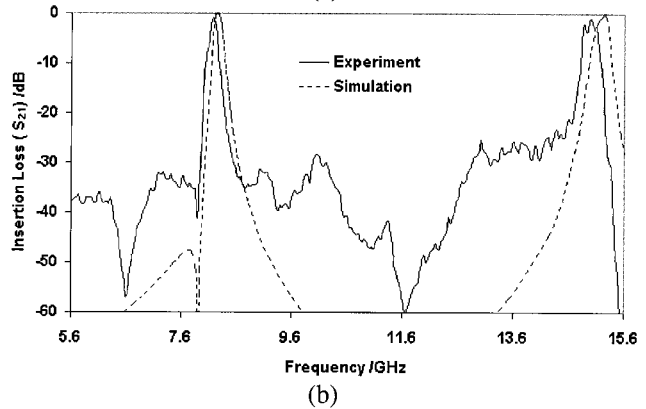
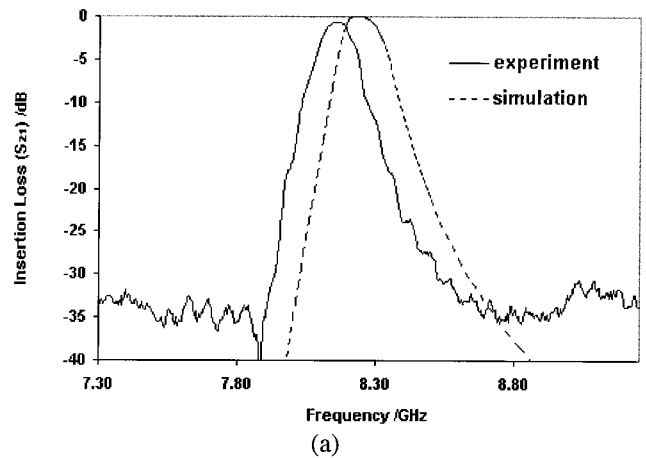


**Figure 8** (a) Passband and (b) wide band of the measured and simulated responses of the Butterworth filter

(1.12%) lower than the simulated one. The measurements (not shown here) at 65 K have a difference of 280 MHz (3.5%), and the simulator does not distinguish between the two temperatures in ignoring the kinetic inductance effects. The measured bandwidth is 140 MHz, slightly narrower than the designed 160 MHz. The minimum passband loss is approximately 0.7 dB, which includes the loss in the connectors. The response is for an as-made device. There has been no tuning.

Figure 8(b) gives the wideband responses at 30 K. As seen from the figure, unwanted responses appear near the passband. The amplitude is up to  $-28$  dB at 10.2 GHz. The reason for this is that interference exists between the circuit and housing. It is also found in this experiment that grounding of the coplanar circuit is very important to suppress the parasitic peaks, as is mentioned in [18]. The first spurious peak at 15 GHz is just as expected.

### 4. CONCLUSION

By introducing the symmetrical interdigital lines on both sides of the central line, a novel slow-wave CPW structure has been studied, the velocity reduction ( $V_p/c_0$ ) of which is about 0.050. The resonator is not only compact in size, because of the enhanced capacitance density, but also has a high unloaded  $Q$  because of the HTS film. Both theory and experiment of the novel superconducting bandpass filter using a CPW slow-wave resonator are presented in this Letter. The measured results of the three-pole filter are in good agreement with the simulated responses, which indicates the potential of this kind of resonator in planar filter design.

## REFERENCES

1. M.J. Lancaster, F. Huang, A. Porch, B. Avenhaus, J. Hong, and D. Hung, Miniature superconducting filters, *IEEE Trans Microwave Theory Tech* MTT-44(1996), 1339–1346.
2. J.K.A. Everard and K. K.M. Cheng, High performance direct coupled bandpass filters on coplanar waveguide, *IEEE Trans Microwave Theory Tech* MTT-41(1993), 1568–1573.
3. K. Hettak, N. Dib, A. Omar, G.Y. Delisle, M. Stubbs, and S. Toutain, A useful new class of miniature CPW shunt stubs and its impact on millimeter-wave integrated circuits, *IEEE Trans Microwave Theory Tech* MTT-47 (1999), 2340–2349.
4. Y.K. Kuo, C.H. Wang, and C.H. Chen, Novel reduced-size coplanar waveguide bandpass filters, *IEEE Microwave Wireless Components Lett* 11 (2001), 65–67.
5. T.M. Weller, Edge-coupled coplanar waveguide bandpass filter design, *IEEE Trans Microwave Theory Tech* MTT-48 (2000), 2453–2458.
6. J.M. Vargas, P. Brown, T. Khan, Y. Hijazi, Y.A. Vlasov, and G.L. Larkins, Jr., Superconducting half-wave microwave resonator on YSZ buffered Si (100), *IEEE Trans Appl Supercond* AS-11 (2001), 392–394.
7. A. Gorur, C. Darpuz, and M. Alkan, Characteristics of periodically loaded CPW structures, *IEEE Microwave Guided Wave Lett* MGW-8 (1998), 278–280.
8. E.H. Bottcher, H. Pfitzenmaier, E. Droge, and D. Bimberg, Millimeter-wave coplanar waveguide slow-wave transmission lines on InP, *Electron Lett* 32 (1996), 1377–1378.
9. H. Kanaya, T. Shinto, K. Yoshida, T. Uchiyama, and Z. Wang, Miniaturized HTS coplanar waveguide bandpass filters with highly packed meanderlines, *IEEE Trans Appl Superconductivities*, Vol. 11, No. 1, pp 481–484, Mar 2001.
10. K. Yoshida, K. Sashiyama, S. Nishioka, H. Shinmakage, and Z. Wang, Design and performance of miniaturized superconducting coplanar waveguide filters, *IEEE Trans Appl Supercond* AS-9 (1999), 3905–3908.
11. D.S. Hung and M.J. Lancaster, Superconducting coplanar fractal slow-wave resonator, *IEEE 3rd High Frequency POSTGRAD Colloquium*, 1997.
12. C. Veyres and V.F. Hanna, Extension of the application of conformal mapping techniques to coplanar lines with finite dimensions, *Int J Electron* 48 (1980), 47–56.
13. G. Matthaei, L. Young, and E.M.T. Jones, *Microwave filters, impedance-matching networks and coupling structure*, Artech House, Dedham, MA, 1980.
14. EM User's Manual, Sonnet Software, Inc. Version 6, 1999.
15. R.E. Collin, *Foundation for microwave engineering*, McGraw-Hill, New York, 1992.
16. H.T. Su, F. Huang, and M.J. Lancaster, Highly miniature HTS microwave filters, *IEEE Trans Appl Supercond* AS-11, (2001), 349–352.
17. J. Liang, C. Shih, Q. Huang, D. Zhang, and G. Liang, HTS microstrip filters with multiple symmetric and asymmetric prescribed transmission zeros *IEEE MTT-S Int Microwave Symposium Digest*, 1999, pp1551–1554.
18. S. Uysal, Coplanar waveguide edge-coupled bandpass filters with finite ground planes, *Electron Lett* 33 (1997), 395–376.

© 2002 Wiley Periodicals, Inc.

## MULTIMEDIA APPLICATIONS USING OPTICAL FFH-CDMA COMMUNICATION SYSTEMS

M. Thiruchelvi,<sup>1</sup> M. Meenakshi,<sup>2</sup> and G. Geetha<sup>2</sup>

<sup>1</sup> Department of Electronics and Communication Engineering  
Sri Venkateswara College of Engineering  
Madras University

Chennai, Tamilnadu, India 602105

<sup>2</sup> School of Electronics and Communication Engineering  
Anna University  
Chennai, Tamilnadu, India 600025

Received 14 February 2002

**ABSTRACT:** In this Letter multimedia transmission in an optical-fiber network using a fast frequency hopping–code division multiple access scheme is discussed. The multirate one coincidence variable length frequency hop patterns have been generated and their auto- and cross-correlation properties are studied. A series of multiple Bragg gratings in a single optical fiber has been proposed to implement the encoder and decoder. Bit-error-rate analysis assuming Gaussian approximation for the error probability has been carried out. The results of the numerical analysis reveal that this system can support up to 30 simultaneous users with two different data rates (e.g., 500 Mbps and 2 Gbps). It can be concluded from the results that the fast frequency hopping–optical code division multiple access system is capable of supporting multimedia applications. © 2002 Wiley Periodicals, Inc. *Microwave Opt Technol Lett* 34: 259–263, 2002; Published online in Wiley InterScience (www.interscience.wiley.com). DOI 10.1002/mop.10432

**Key words:** multirate one-coincidence variable-length optical codes; FFH-OCDMA; bit error rate; multiple access interference

### 1. INTRODUCTION

Optical code division multiple access (OCDMA) communication systems have many advantages in addition to their large bandwidth. The bandwidth can be utilized more efficiently by multirate transmission needed for multimedia application. In multirate transmission both the lower and higher ends of the frequency spectrum are utilized at the same time, and the frequency hopping–OCDMA scheme helps to reduce the multiple access interference (MAI), when compared to other direct sequence spread spectrum methods.

In Section 2, the optical FFH-OCDMA system is described, and the multirate code design is explained in Section 3. In Section 4, bit error rate (BER) is evaluated. The numerical analysis is carried out in Section 5, and the conclusion is given in Section 6.

### 2. SYSTEM DESCRIPTION OF OPTICAL FAST FREQUENCY HOP-CODE DIVISION MULTIPLE ACCESS SYSTEMS

In a fast frequency hop–optical code division multiple access (FFH-OCDMA) system, the available bandwidth is subdivided into a large number of continuous frequency slots, and each user is assigned a unique frequency hop pattern as their own address sequence. Each pulse in the address sequence is transmitted at a different wavelength.

In the proposed FFH system, the modulator transmits power in the chip interval if the chip value is one, otherwise no power is transmitted. The encoder/decoder is implemented by the series of Bragg grating in a single fiber, and all the gratings are written to the same wavelength but can be tuned independently to the given wavelength with the use of piezoelectric devices. The series of multiple gratings will spectrally and temporally slice an incoming broadband pulse into several components [1]. The architecture of encoder and decoder are shown in Figure 1. Each grating in the series of gratings reflects one pulse of duration ( $T_c$ ) corresponding